

## Sb<sub>2</sub>Se<sub>3</sub> sensitized heterojunction solar cells

Anil N. Kulkarni<sup>2</sup> · Sandeep A. Arote<sup>1</sup> · Habib M. Pathan<sup>1</sup> · Rajendra S. Patil<sup>2</sup>

Received: 26 February 2015 / Accepted: 29 July 2015 / Published online: 15 August 2015  
© The Author(s) 2015. This article is published with open access at Springerlink.com

**Abstract** The study deals with the sensitization of the porous SnO<sub>2</sub> films deposited on fluorine-doped tin oxide with nanocrystalline Sb<sub>2</sub>Se<sub>3</sub>. The sensitization was achieved for three different sensitization times employing chemical solution deposition with antimony chloride and sodium selenosulphate as precursors for Sb<sup>3+</sup> and Se<sup>2-</sup>, respectively. The unsensitized and sensitized photoelectrodes were characterized using X-ray diffractometry, scanning electron microscopy and diffused reflectance spectroscopy. The solar cells fabricated using three different photoelectrodes were characterized for their photovoltaic performance using the photocurrent density versus photovoltage curves. The study revealed that sensitization time significantly influences the photovoltaic parameters namely, short circuit current density ( $J_{sc}$ ), open circuit voltage ( $V_{oc}$ ) and fill factor (FF) and hence the photovoltaic efficiency ( $\eta$ ).

**Keywords** Sb<sub>2</sub>Se<sub>3</sub> · Photosensitization · SnO<sub>2</sub> · Heterojunction · Solar cell

### Introduction

Metal chalcogenides such as CdS [1], CdSe [2], Ag<sub>2</sub>S [3], Sb<sub>2</sub>S<sub>3</sub> [4], Bi<sub>2</sub>S<sub>3</sub> [5] and Sb<sub>2</sub>Se<sub>3</sub> [6] have recently attracted considerable attraction of researchers due to their potential applications in electrical and optical devices. Among these materials, antimony selenide (Sb<sub>2</sub>Se<sub>3</sub>) is a group V<sub>2</sub>–VI<sub>3</sub> layered structured direct band gap semiconductor with orthorhombic crystal structure [7]. Sb<sub>2</sub>Se<sub>3</sub> displays a narrow band gap of 1.1–1.3 eV, [8–10] which approaches the ideal Shockley–Queisser value, [11] and has the ability to extend light harvesting over the near-IR region up to approximately 1000 nm. Besides, the relative positions of the conduction band edges of nanostructured Sb<sub>2</sub>Se<sub>3</sub> and SnO<sub>2</sub> display favourable energetics for electron transfer at their interface [12]. In addition, theoretical calculations performed by Giustino et al. [9, 10] demonstrated the improved performance of Sb<sub>2</sub>Se<sub>3</sub>-based devices compared to Sb<sub>2</sub>S<sub>3</sub> based cells, and suggested Sb<sub>2</sub>Se<sub>3</sub> as a promising candidate for achieving 20 % PCE. In spite of these advantages, Sb<sub>2</sub>Se<sub>3</sub>-based solar cells have rarely been experimentally demonstrated. Of these one is photoelectrical solar cell fabricated using a Sb<sub>2</sub>Se<sub>3</sub> photoanode prepared by chemical bath deposition (CBD) reported by Bhattacharya et al. [13]. Second one is based on electrodeposited Sb<sub>2</sub>Se<sub>3</sub> thin films in TiO<sub>2</sub>/Sb<sub>2</sub>Se<sub>3</sub>/CuSCN planer heterojunction solar cells reported by Zaera et al. [14]. However, only one report is available on photovoltaic performance of Sb<sub>2</sub>Se<sub>3</sub> as a sensitizer spin coated on TiO<sub>2</sub> photoanode in semiconductor sensitized solar cell applications [6]. Conversely, the reports available on Bi<sub>2</sub>S<sub>3</sub> and Sb<sub>2</sub>S<sub>3</sub> sensitized SnO<sub>2</sub> photoanode-based solar cells are limited [4, 5], which showed very low power conversion efficiency (PCE) as compared to other nanocrystalline semiconductor sensitized solar cells. Till date, TiO<sub>2</sub> has

✉ Anil N. Kulkarni  
kulkarni.may29@gmail.com

<sup>1</sup> Advanced Physics Laboratory, Department of Physics, Savitribai Phule University, Pune 411007, India

<sup>2</sup> Department of Physics, PSGVPM's ASC College, Shahada, India.

widely been used as photoanode material in most of the SSSCs [1–5]. However, the promising optical and electrical properties of  $\text{SnO}_2$ , such as higher electronic mobility and large band gap (3.8 eV), draw the attention of researchers towards it as an alternative photoanode for SSSC. Furthermore,  $\text{SnO}_2$  has a 0.4 V more positive band edge as compared to  $\text{TiO}_2$ ; hence, effective charge injection into  $E_{\text{CB}}$  of  $\text{SnO}_2$  from excited sensitizer is expected compared to  $\text{TiO}_2$  [12]. In spite of merits of these semiconductor materials for its solar cell application, reasons for the low conversion efficiencies of cells based on stibnite family members still elude better understanding. Studies on different factors responsible for the photoconversion in these cells need to be carried out and optimized for obtaining the theoretically projected efficiencies of these nanostructured excitonic solar cells. Therefore, to investigate the effect of various parameters such as photoanode properties, counter electrode, electrolyte and sensitization time of photoanode, which decide performance of cells based on  $\text{Sb}_2\text{Se}_3$  still need further studies and optimization.

In this work, porous  $\text{SnO}_2$  photoelectrodes have been prepared by doctor blade method. Sensitization of  $\text{SnO}_2$  photoelectrode with nanocrystalline  $\text{Sb}_2\text{Se}_3$  has been achieved using chemical bath deposition by varying the sensitization time from 30 to 120 min. To the best of our knowledge, first time we are exploring the  $\text{SnO}_2/\text{Sb}_2\text{Se}_3$  combination in semiconductor sensitized solar cells and of the many influencing factors, the effect of sensitization time is given emphasis in the present study.

## Experimental

### Materials

All chemicals [antimony chloride ( $\text{SbCl}_3$ ) (Merck), sodium sulphite (SRL), selenium metal powder (Thomas baker), triethanolamine (TEA) (SRL)] were of the highest purity available and they were used without further purification.

### Preparation of $\text{SnO}_2$ photoanode

To make  $\text{SnO}_2$  paste, 0.5 gm of  $\text{SnO}_2$  powder was mixed with ethanol, acetic acid, ethylene glycol and  $\alpha$ -terpineol in mortar and pestle for 40 min, then  $\text{SnO}_2$  film was prepared on fluorine-doped tin oxide (FTO) glass by doctor blade method. After drying, all samples were annealed at 450 °C for 1 h.

### Chemical bath deposition of $\text{Sb}_2\text{Se}_3$ on porous $\text{SnO}_2$ photoanode

In the present synthesis, solutions of  $\text{SbCl}_3$  (0.01 M; 10 ml) and  $\text{Na}_2\text{SeSO}_3$  (0.01 M; 10 ml) were prepared in acetone

and double distilled water, respectively, in two different beakers, wherein  $\text{SbCl}_3$  acts as a precursor of  $\text{Sb}^{3+}$  and  $\text{Na}_2\text{SeSO}_3$  that of  $\text{Se}^{2-}$ . TEA (20 %; 5 ml), a complexing agent, was then added to the bath containing antimony source. The solution containing selenium source was then slowly added to the bath containing  $\text{Sb}^{3+}$  and TEA. The deposition process of  $\text{Sb}_2\text{Se}_3$  was considered to be based on slow release of  $\text{Sb}^{3+}$  and  $\text{Se}^{2-}$  ions in the solution, which was achieved using TEA. TEA controls the  $\text{Sb}^{3+}$  ion concentration and allows for obtaining soluble species of  $\text{Sb}^{3+}$  in the bath. The pH of the combined bath was adjusted to be around 8–10, by adding few drops of 1 M NaOH solution. The previously prepared  $\text{SnO}_2$  photoelectrodes were introduced vertically into this bath containing both  $\text{Sb}^{3+}$  and  $\text{Se}^{2-}$ , at room temperature for the deposition of  $\text{Sb}_2\text{Se}_3$  over the porous nanocrystalline  $\text{SnO}_2$ . After carrying out sensitization for different time durations of about 30, 60 and 120 min, the photoelectrodes were withdrawn from the bath and the corresponding photoanodes were named as P-30, P-60 and P-120, respectively. The sensitized photoelectrodes were observed to be coated with increased darkening of brownish tinge of the photoanodes from P-30 to P-120. This may be due to the enhanced level of deposition of nanocrystalline  $\text{Sb}_2\text{Se}_3$  onto the bare photoanodes of  $\text{SnO}_2$  with increase in sensitization time.

## Solar cell assembly

### Preparation of electrolyte and counter electrode

- Electrolyte: The aqueous solution of polysulphide electrolyte was prepared using the 0.5 M  $\text{Na}_2\text{S}$ , 0.1 M sulfur powder and 0.2 M KCl.
- Counter electrode: To prepare the counter electrode, the FTO glass was washed with acetone, water, and ethanol. After removing contaminants, carbon-coated counter electrode was prepared on the conductive side of the FTO substrate using mild flame.

For cell assembly, the carbon-coated FTO was used as a counter electrode. The  $\text{Sb}_2\text{Se}_3$  sensitized  $\text{SnO}_2$  photoelectrode and counter electrode were clamped together into a sandwich type configuration with a droplet of polysulphide electrolyte injected between them. The fabricated solar cells using photoelectrodes P-30, P-60 and P-120 were named C-30, C-60 and C-120, respectively, and characterized to study their photovoltaic performance.

The analysis of structural, morphological properties and elemental composition of unsensitized  $\text{SnO}_2$  photoanode and  $\text{Sb}_2\text{Se}_3$  sensitized photoanode of  $\text{SnO}_2$  was carried out using X-ray diffractometry (XRD) (model: XRD, Rigaku “ $D/B_{\text{max}} - 2400$ ”,  $\text{Cu } K_{\alpha} = 0.154$  nm), scanning electron microscopy (SEM) (model: JEOL-JSM 6360-A) and

energy-dispersive X-ray spectroscopy (EDAX), respectively. A UV–Vis spectrophotometer (model: JASCO V-670) was used to record optical absorption spectra of unsensitized and sensitized photoelectrodes in diffused reflectance mode in the range 200–800 nm at room temperature. The cell performance was measured by a semiconductor characterization unit [Keithley 2420 (source meter)] under illumination of  $30 \text{ mW cm}^{-2}$ .

## Results and discussions

### Structural analysis of bare $\text{SnO}_2$ and $\text{SnO}_2/\text{Sb}_2\text{Se}_3$ photoanodes

Figure 1 shows diffraction pattern for unsensitized  $\text{SnO}_2$  photoelectrode with defined peaks at  $2\theta = 26.63^\circ$ ,  $34.07^\circ$ ,  $38.20^\circ$ ,  $52.18^\circ$  and  $55.19^\circ$  corresponding to the diffraction from planes which confirm its tetragonal phase (JCPDS file no: 41-1445). Figure 1 also shows the diffraction patterns related to P-10, P-20 and P-30, respectively. P-30, P-60 and P-120 show diffraction signatures corresponding to both,  $\text{Sb}_2\text{Se}_3$  and  $\text{SnO}_2$ . In P-30, P-60 and P-120,  $\text{Sb}_2\text{Se}_3$  nanocrystals appeared in the orthorhombic phase (JCPDS file no: 72-1184).

### Optical properties of bare $\text{SnO}_2$ and $\text{SnO}_2/\text{Sb}_2\text{Se}_3$ photoanodes

The absorption spectra of the unsensitized  $\text{SnO}_2$ , P-30, P-60 and P-120 are shown in Fig. 2. It is seen from the figure that the absorption for unsensitized  $\text{SnO}_2$  is limited to the ultraviolet region of electromagnetic spectrum.

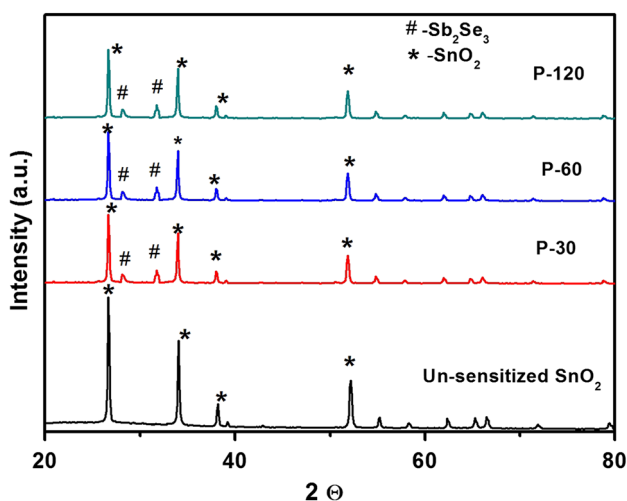


**Fig. 1** XRD spectra of bare  $\text{SnO}_2$  and  $\text{SnO}_2/\text{Sb}_2\text{Se}_3$  photoanodes sensitized with different deposition times; P-30: 30 min, P-60: 60 min and P-120: 120 min

However, for all sensitized photoelectrodes, the absorbance is enhanced in the visible region. It may be noted that the intensity of the absorption spectra increases in the visible region from 400 to 600 nm with the increasing sensitization time from P-30 to P-120. This fact suggests that amount of loading of a sensitizer increases with increase of loading time resulting in enhanced absorption of visible light from P-30 to P-120. Also, there is an apparent red shift in the absorption feature from P-30 to P-120, which is probably a consequence of increase in particle size of sensitizer with increase of deposition time and may be attributed to the aggregation of sensitizer on the surface of bare photoelectrode. This observation is in accordance with the other metal chalcogenides including  $\text{Sb}_2\text{Se}_3$  deposited with SILAR technique [9, 16].

### Morphological and elemental analysis of $\text{SnO}_2/\text{Sb}_2\text{Se}_3$ photoanodes

To further analyse the effect of sensitization time on the  $\text{SnO}_2$  photoelectrode, morphology of both bare and sensitized photoelectrode was studied. Figure 3 shows the scanning electron micrographs of  $\text{Sb}_2\text{Se}_3$  sensitized  $\text{SnO}_2$  photoelectrode with different sensitization times. It is clearly seen from Fig. 3 that the pores in  $\text{SnO}_2$  photoelectrode are filled up with nanocrystalline  $\text{Sb}_2\text{Se}_3$ . The pore-filling apparently increased with increase of deposition time from P-30 to P-120. In addition to this, there is no observable alteration in the surface quality and structure of the  $\text{SnO}_2$  photoelectrodes with the increase in sensitization time.

Supplementary elemental analysis by energy-dispersive X-ray spectroscopy (EDAX) for unsensitized and sensitized photoelectrode was carried out and shown in Fig. 4. EDAX spectrum for unsensitized film reveals the presence of only Sn and O, while that of all sensitized films show the presence of Sb and S in addition to Sn and O. The quantitative analysis obtained by EDAX shows an overall increment in the amount of Sb and Se from P-30 to P-120, with increasing deposition time. It is also observed that Sb/Se ratio leads to the average stoichiometric value of 2/3 for sensitization time of 120 m (Table 1). Therefore, the XRD results along with EDAX spectrum analysis demonstrate sensitization of  $\text{SnO}_2$  qualitatively using CBD.

### Photovoltaic performance analysis

The photovoltaic performance of solar cells C-30, C-60 and C-120 was investigated by conducting photocurrent density ( $J$ ) versus voltage ( $V$ ) measurements. Figure 5 shows photocurrent density ( $J$ ) versus photovoltage ( $V$ ) characteristics curves of the fabricated solar cells namely, C-30 and C-60. The photovoltaic parameters like short circuit

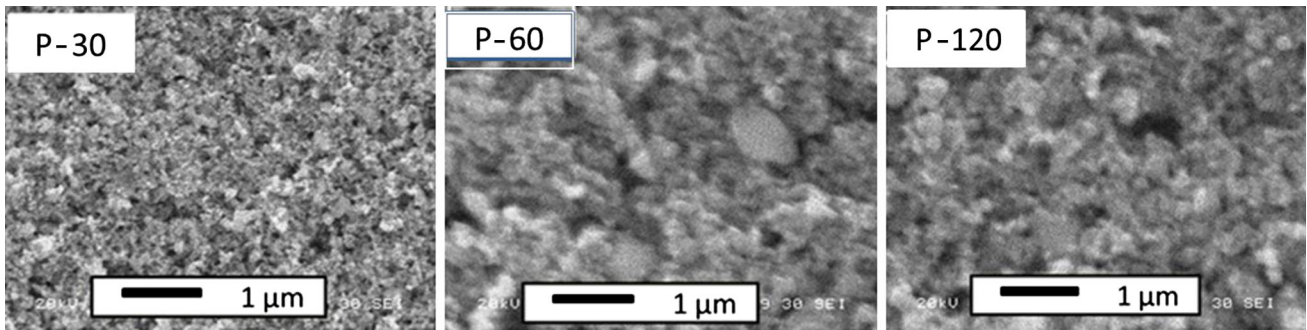


**Fig. 2** Optical absorption spectra of bare SnO<sub>2</sub> and SnO<sub>2</sub>/Sb<sub>2</sub>Se<sub>3</sub> photoanodes sensitized with different deposition times; P-30: 30 min, P-60: 60 min and P-120: 120 min

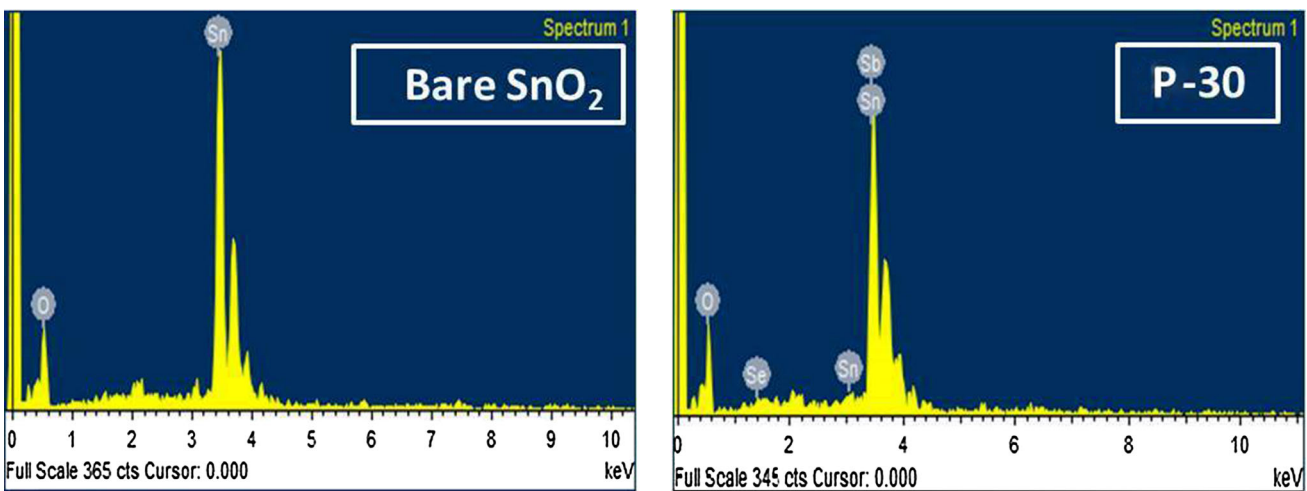


**Fig. 3** Elemental (% atomic) analysis of bare SnO<sub>2</sub> and SnO<sub>2</sub>/Sb<sub>2</sub>Se<sub>3</sub> photoanodes sensitized for 30 min

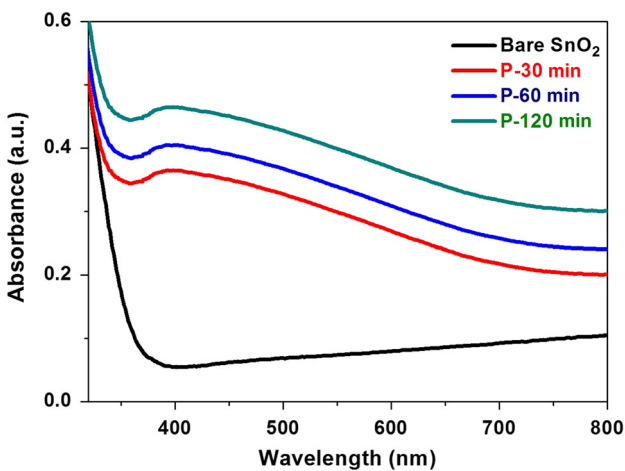


**Fig. 4** SEM images of SnO<sub>2</sub>/Sb<sub>2</sub>Se<sub>3</sub> photoanodes sensitized with different deposition times; P-30: 30 min, P-60: 60 min and P-120: 120 min

**Table 1** Elemental (% atomic) analysis of bare SnO<sub>2</sub> and SnO<sub>2</sub> photoanodes sensitized with Sb<sub>2</sub>Se<sub>3</sub>

Photoanode	Sensitization time (min)	Sn	O	Sb	Se
Bare SnO <sub>2</sub>	–	39.97	60.03	–	–
P-30	30	24.32	73.64	1.08	0.96
P-60	60	21.84	65.63	5.43	7.10
P-120	120	21.05	62.89	6.02	10.04

current density ( $J_{sc}$ ), open circuit voltage ( $V_{oc}$ ), fill factor (FF) and photovoltaic efficiency ( $\eta$ ) are obtained from the J–V curves and listed in Table 2.

It is observed from the Table 2 that, with increase in sensitization time, the value of  $J_{sc}$  increases, while  $V_{oc}$  shows decrease in its value from C-30 to C-60. However, in spite of better optical absorbance of P-120 vis-à-vis others, cell fabricated using it does not show considerable photovoltaic performance. This may be due to the over aggregation of sensitizer over the surface of the photoanode.

With increase of sensitization time, the optical absorption spectra as given in Fig. 2 clearly show an enhanced amount of loading of the sensitizer into the

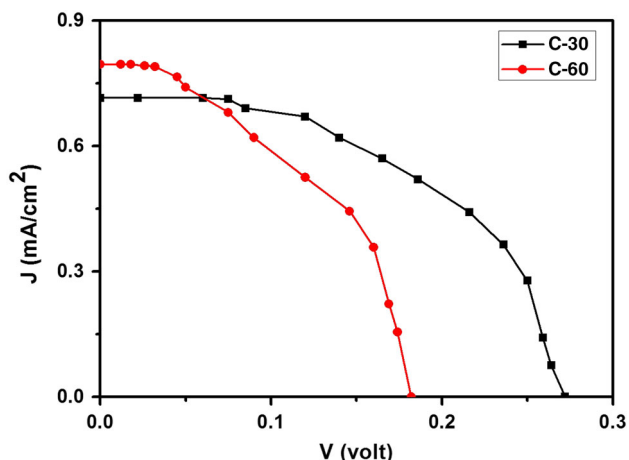


**Fig. 5** J-V characteristics of cells C-30 and C-60 fabricated with SnO<sub>2</sub>/Sb<sub>2</sub>Se<sub>3</sub> photoanodes sensitized with deposition times of 30 and 60 min, respectively

**Table 2** Photovoltaic parameters of Sb<sub>2</sub>Se<sub>3</sub> sensitized SnO<sub>2</sub> photoanode-based solar cell prepared with different sensitization time

Solar cell	Sensitization time (min)	V <sub>oc</sub> (V)	J <sub>sc</sub> (mA/cm <sup>2</sup> )	FF (%)	η (%)
C-30	30	0.272	0.715	49	0.31
C-60	60	0.182	0.795	41	0.19

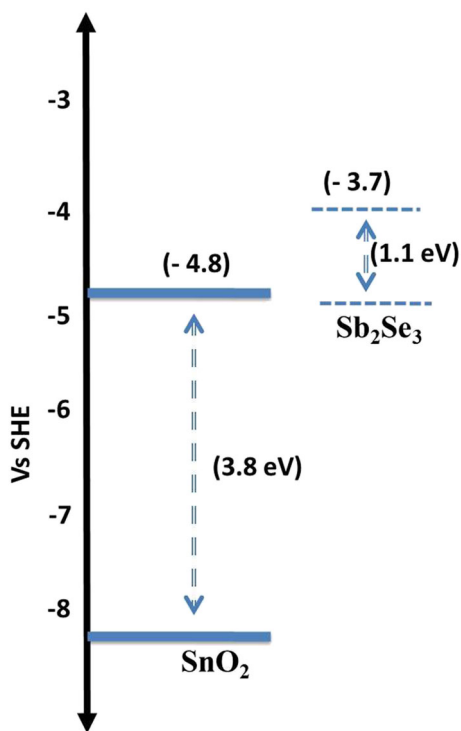


**Fig. 6** Schematic showing band energetics of SnO<sub>2</sub>/Sb<sub>2</sub>Se<sub>3</sub> interface

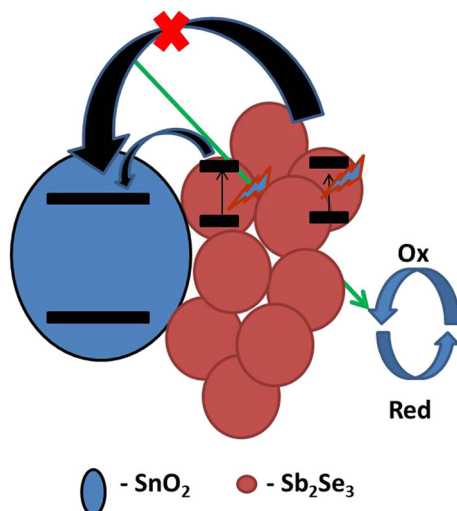


**Fig. 7** Cartoon showing recombination of excited electron at SnO<sub>2</sub>/Sb<sub>2</sub>Se<sub>3</sub>-electrolyte interface due to aggregation

photoelectrodes. This is evident from the improved optical absorption in the visible region. Such an enhanced absorption of light in the visible region leads to generation of increased number density of excitons at the electrode–electrolyte interface. The excitons so generated get dissociated at the SnO<sub>2</sub>/Sb<sub>2</sub>Se<sub>3</sub> interface due to the favourable interfacial band energetics (see Fig. 6) leading to effective electron injection from excited Sb<sub>2</sub>Se<sub>3</sub> to the conduction band of SnO<sub>2</sub> [15], which further results in improved photocurrent (*J*) from C-30 to C-60 and hence *J*<sub>sc</sub> in from C-30 to C-60.

But, such an aggregation of sensitizer may cause to delay the transfer of excited electrons from sensitizer to the conduction band of SnO<sub>2</sub>, giving rise to the recombination of excited electron at electrode–electrolyte interface. This probable reason depicted in schematic form in Fig. 7 apparently explains the reduction of V<sub>oc</sub>, for C-60.

However, as discussed earlier in optical analysis, optical absorption enhances with increase in deposition time, which may be attributed to the further aggregation of sensitizer in P-120. In spite of enhanced absorption in P-120, the increased number density of sensitizer molecules in it, may have offered the increased grain boundary resistance in C-120 vis-a-vis former, probably affected the photocurrent (*J*) and photovoltage (*V*). This probable reason depicted in schematic form in Fig. 7, which apparently rationalizes the poor values of photovoltage and photocurrent in C-120 and hence not incorporated in the Table 2. The same was confirmed by the Solis and Co-Workers [16].

Relatively better photovoltaic efficiency of C-30 vis-a-vis other cells may be obviously attributed to its improved photovoltaic parameters.

The performance observed in present study in terms of photoconversion efficiency ( $\eta$ ) about 0.31 % is relatively greater than that of as-prepared spin-coated TiO<sub>2</sub> photoanode with Sb<sub>2</sub>Se<sub>3</sub>-based solar cell showing efficiency of about 0.22 % reported by Seok et al. [6]. It can be seen from Fig. 6, showing band energetics of SnO<sub>2</sub>/Sb<sub>2</sub>Se<sub>3</sub> interface, that conduction band ( $E_{CB}$ ) of Sb<sub>2</sub>Se<sub>3</sub> lies well above the  $E_{CB}$  of SnO<sub>2</sub>; hence, effective charge injection into  $E_{CB}$  of SnO<sub>2</sub> from excited Sb<sub>2</sub>Se<sub>3</sub> is expected as compared to TiO<sub>2</sub> [12]. This may be one of the probable reasons that Sb<sub>2</sub>Se<sub>3</sub> in combination with SnO<sub>2</sub> shows better performance. This suggests SnO<sub>2</sub>, potential alternative to conventional TiO<sub>2</sub>-based system in SSSC.

## Conclusions

In the present report, we have demonstrated the photovoltaic performance of Sb<sub>2</sub>Se<sub>3</sub> sensitized SnO<sub>2</sub>-based solar cells. The optical, morphological properties and photovoltaic characteristics of SnO<sub>2</sub>/Sb<sub>2</sub>Se<sub>3</sub> photoanodes were analysed as a function of sensitization time. From the study, it may be concluded that sensitization time has a profound influence on all the photovoltaic parameters, thus, effecting the photoconversion efficiency of these cells. It is understood that the overall efficiency of a nanostructured solar cell may be improved by developing a conformal monolayer coating of sensitizer as this can improve the light harvesting efficiency besides mitigating the back electron transfer.

HMP is thankful to Departmental Research Development program, Savitribai Phule Pune University, Pune—07 for partial financial support. ANK is grateful to Prof. M. B. Rajendra Prasad for discussions during drafting to raise the quality of English and to make manuscript informative.

**Open Access** This article is distributed under the terms of the Creative Commons Attribution 4.0 International License (<http://creativecommons.org/licenses/by/4.0/>), which permits unrestricted use, distribution, and reproduction in any medium, provided you give appropriate credit to the original author(s) and the source, provide a link to the Creative Commons license, and indicate if changes were made.

## References

1. Sun, W., Yu, Y., Pan, H., Gao, X.F., Chen, Q., Peng, L.M.: CdS quantum dots sensitized TiO<sub>2</sub> nanotube-array photoelectrodes. *J. Am. Chem. Soc.* **130**, 1124–1125 (2008)

2. Chen, Y.X., Wei, L., Zhang, G.H., Jiao, J.: Open structure ZnO/CdSe core/shell nanoneedle arrays for solar cells. *Nanoscale Res. Lett.* **7**, 516–521 (2012)
3. Chen, C., Xie, Y., Ali, G., Yoo, S.H., Cho, S.O.: Improved conversion efficiency of Ag<sub>2</sub>S quantum dot-sensitized solar cells based on TiO<sub>2</sub> nanotubes with a ZnO recombination barrier layer. *Nanoscale Res. Lett.* **6**, 462–470 (2011)
4. Kulkarni, A.N., Arote, S.A., Pathan, H.M., Patil, R.S.: Room temperature synthesis of crystalline Sb<sub>2</sub>S<sub>3</sub> for SnO<sub>2</sub> photoanode-based solar cell application. *Bull. Mater. Sci.* **38**, 493–498 (2014)
5. Kulkarni, A.N., Arote, S.A., Pathan, H.M., Patil, R.S.: Time dependent synthesis of crystalline Bi<sub>2</sub>S<sub>3</sub> and its application as a sensitizer in SnO<sub>2</sub> based solar cells. *Int. J. Mater. Res.* **105**, 314–317 (2014)
6. Choi, Y., Mandal, T., Yang, W., Lee, Y., HyukIm, S., Noh, J., Seok, S.: Sb<sub>2</sub>Se<sub>3</sub>-sensitized inorganic-organic heterojunction solar cells fabricated using a single-source precursor. *Angew. Chem.* **53**, 1329–1333 (2014)
7. Ko, T.Y., Sun, K.W.: Optical and electrical properties of single Sb<sub>2</sub>Se<sub>3</sub> nanorod. *J. Lumin.* **129**, 1747–1749 (2009)
8. Platakis, N.S., Gatos, H.C.: Threshold and memory switching in crystalline chalcogenide materials. *Phys. Status Solidi A Appl. Res.* **13**, K1 (1972)
9. Patrick, C.E., Giustino, F.: Structural and electronic properties of semiconductor-sensitized solar-cell interfaces. *Adv. Funct. Mater.* **21**, 4663–4667 (2011)
10. Filip, M.R., Patrick, C.E., Giustino, F.: G W quasiparticle band structures of stibnite, antimonselite, bismuthinite, and guanajuatite. *Phys. Rev. B* **87**, 205125 (2013)
11. Shockley, W., Queisser, J.: Detailed balance limit of efficiency of *p-n* junction solar cells. *J. Appl. Phys.* **32**, 510–519 (1961)
12. Rhee, J.H., Chung, C., Wei-Guang Diao, E.: A perspective of mesoscopic solar cells based on metal chalcogenide quantum dots and organometal-halide perovskites. *NPG Asia Mater.* **5**, e68 (2013)
13. Bhattacharya, R.N., Pramanik, P.: A photoelectrochemical cell based on chemically deposited Sb<sub>2</sub>Se<sub>3</sub> thin film electrode and dependence of deposition on various parameters. *Sol. Energy Mater.* **6**, 317–322 (1982)
14. Tuyen Ngo, T., Chavhan, S., Kosta, I., Miguel, O., Grande, H., Tena-Zaera, R.: Electrodeposition of antimony selenide thin films and application in semiconductor sensitized solar cells. *Appl. Mater. Interfaces* **6**, 2836–2841 (2014)
15. Guijarro, N., Lana-Villarreal, T., Shen, Q., Toyoda, T., Gomez, R.: Sensitization of titanium dioxide photoanodes with cadmium selenide quantum dots prepared by SILAR: photochemical and carrier dynamics studies. *J. Phys. Chem. C* **114**, 21928–21937 (2010)
16. Solis, M., Rincon, M.E., Calva, J.C., Alvarado, G.: Bismuth sulfide sensitized TiO<sub>2</sub> arrays for photovoltaic applications. *Electrochem. Acta* **112**, 159–163 (2013)